

Development of a Radiation Shielding Monte Carlo Code: RShieldMC

Shenshen GAO^{1,2}, Zhen WU^{1,3}, Xin WANG^{1,2}, Rui QIU^{1,2}, Chunyan LI^{1,3}, Wei LU^{1,2}, Junli LI^{1,2*},

1. Department of Physics Engineering, Tsinghua University, Beijing, China, 100084;

2. Key Laboratory of Particle & Radiation Imaging (Tsinghua University), Ministry of Education, Beijing China, 100084)

3. Nuctech Company Limited, Beijing, China, 10084

* Corresponding Author, E-mail : lijunli@tsinghua.edu.cn

Abstract - Monte Carlo method can simulate the particle behavior accurately. But low efficiency of Monte Carlo calculation and geometry modeling restricts its wide application in the field of radiation shielding. This paper developed a coupled neutron/photon/electron transport Monte Carlo code called RShieldMC, especially for the radiation shielding calculation. It is intended to solve the efficiency and geometry modeling in radiation shielding calculation. Two variance reduction techniques, CNP-AIS (Completely Coupled Neutron-Photon Auto-Importance Sampling Method) and FPAIS (Forced Pointing Auto-Importance Sampling) were developed to solve the deep penetration problem and complex shielding problem. The BREP→CSG conversion method was developed to realize the efficient modeling Monte Carlo geometry. RShieldMC can also provide the hybrid rendering of three-dimensional dose field. Validation results shown in this paper prove the capabilities of RShieldMC in radiation shielding problems with good performances.

I. INTRODUCTION

The design and analysis of the radiation shielding system are important to the safety of nuclear facilities. Along with the development of nuclear power and nuclear technology, the requirement of refined shielding calculation is increasing. Monte Carlo method can simulate the particle behavior accurately. Compared with other methods, it has incomparable advantages in calculation accuracy, completeness of the physical model, ability of geometric descriptions and so on. In addition, with the rapid development of high performance computer, Monte Carlo method has attracted more and more attentions in the design and analysis of radiation shielding system.

The critical bottleneck that restricts the wide application of Monte Carlo method in the field of radiation shielding calculation is efficiency of Monte Carlo calculation and geometry modeling. Although there are various Monte Carlo codes that were developed by different research institutions worldwide, there is still a lack of pertinence in solving efficiency and geometry modeling in radiation shielding calculation. In this study, a new coupled neutron/photon/electron Monte Carlo transport code called RShieldMC (Radiation Shield Monte Carlo Code) has been developed by Department of Engineering Physics, Tsinghua University, Beijing. RShieldMC intends to solve the deep penetration problem, complex shielding problem and improve the efficiency of geometry modeling. In this paper, the functions of RShieldMC are introduced in Section 2. Some validation results are shown in Section 3.

II. DESCRIPTION OF THE ACTUAL WORK

1. Basic Functions

A. Input and Output

RShieldMC expands the GDML (Geometry Description Markup Language) file based on the XML specification, including geometry, materials, sources, tallies, geometry importance and so on. This expanded GDML file forms the input of RShieldMC. Two assistant tools are implemented in RShieldMC to help users write the input file. One is the JLAMT (J Large-scale Auto Modeling Tool), which is a Monte Carlo geometry modeling software and provides a 3D visualization interactive interface. User can also edit material information and check geometry validation in JLAMT. The other tool can convert CAD (Computer Aided Design) geometry to Monte Carlo geometry automatically, which will be explained in detail in the following section.

One 3D visualization tool is developed to show the output of RShieldMC. It provides hybrid rendering of the geometries and dose field, as shown in Fig.1. It was developed based on the VTK (Visualization Toolkit)¹ library. It can give the 3D and 2D view of geometries and dose field. The dose contour lines can also be added.

B. Geometry treatment

The geometry of RShieldMC is represented by constructive solid geometry (CSG) and the ray tracing acceleration algorithm is used to improve the efficiency of geometric operations. There are three types of geometric elements: Basic Solid, Material Solid, Tree Solid. The Basic Solids supported by RShieldMC include parallelepiped, sphere, cylinder, cone, ring and so on. Basic Solid can be Boolean to each other to form a more complex Basic Solid.

Material Solid contains material and other properties. Tree Solid contains the parent-children relationship and relative position information. RShieldMC supports repeated geometry.

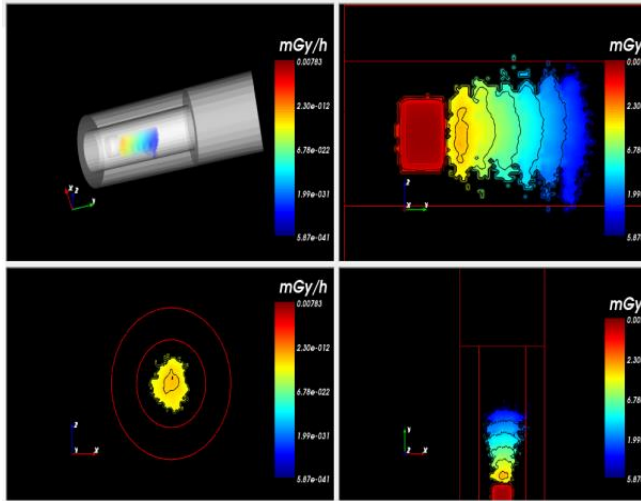


Fig.1. the view of the 3D visualization tool

C. Physics

The coupled neutron/photon/electron transport are supported by RShieldMC. The user can specify the physics model that identify which particles are transported and which reactions are considered.

The following neutron reaction are implemented in RShieldMC: elastic scattering, inelastic scattering, capture and fission. Capture is treated in one of two ways: analog or implicit where the latter is the default model. Generation of photons are optional. Photons are generated if the problem is a combined neutron/photon or neutron/photon/electron run and if the collision nuclide has a nonzero photon production cross section.

Photoelectric effect, Compton scattering, pair production and photonuclear reaction are available for photon. The thick-target bremsstrahlung model (TTB) is optional for acceleration which assumes that generated electrons are locally slowed to rest and banks bremsstrahlung photons produced by the non-transported electrons for later transport.

In RShieldMC, electron transport is modeled by the class II condensed history simulation scheme with a continuous slowing down approximation. Energy straggling and multiple scattering are modeled.

The cross sections used in RShieldMC are generated from raw ENDF/B data and stored in the ACE format.

D. Tallies

RShieldMC register the detector, which contains tally types and other information, for the Tree Solid to connect the geometry and tally. The following tally functions are

available in RShieldMC: cell flux, surface flux, surface current, point flux, energy deposit. In addition, A Chinese reference human (male/female) dose conversion factor database, which converts the neutron/photon flux to an effective dose, is embedded in RShieldMC. So RShieldMC can give effective dose for staff dose assessment².

2. Variance Reduction Techniques

Some common variance reduction techniques including geometry importance, point detector are implemented in RShieldMC. In addition, two new variance reduction techniques, called CNP-AIS (Completely Coupled Neutron-Photon Auto-Importance Sampling Method) and FPAIS (Forced Pointing Auto-Importance Sampling Method) have been developed specifically to solve the deep penetration problem and complex shielding problem, like the maze shielding calculation.

A. CNP-AIS Method

CNP-AIS³ method is an improved Auto-Importance Sampling (AIS) method⁴ proposed by Tsinghua University for deep penetration problems. CNP-AIS method is based on next event estimators and biased sampling. It can automatically adjust the particle importance distribution while transporting particles in layered space continuously. In general, the CNP-AIS method divides the whole geometry space into $K+1$ sub-spaces by introducing K fictitious surfaces; particles are transported in these sub-spaces in sequence. The fictitious surface k ($k=1,2,\dots,K$) is the Current Fictitious Surface (CFS) of sub-space k . In each sub-space, except for the last sub-space, fictitious particles are created on CFS using next event estimator while transporting source particles and secondary particles. The source particles and secondary particles will be killed if they traverse CFS. After all the source particles are simulated, the weights and number of fictitious particles are automatically adjusted using splitting/Russian roulette until the number of fictitious particles are adjusted to be as many as the source particles. Then, the fictitious particles are set as the source of the next sub-space, and the particle transport is performed in the next sub-space, as shown in Fig. 2.

In coupled neutron/photon transport, the procedure is slightly more complicated than above. In the CNP-AIS method, both neutron and photon fictitious surfaces are introduced. The geometry, type, number and location of the fictitious surface should be determined:

- 1) The geometry of fictitious surface is chosen according to the geometry of the three-dimensional model and the tally region. For instance, the planar fictitious surface is normally used for slab shielding problem; for reactor shielding problem, cylindrical fictitious surface is always used if the tally region is located at the lateral face of the pressure vessel.

2) The fictitious surface type (neutron or photon) is chosen depending on the shielding effect of the material. If the shielding effect of the material is obvious for neutron (or photon), neutron (or photon) fictitious surface should be introduced inside the material; if the material is suitable for both neutron and photon shielding, neutron and photon fictitious surfaces should be introduced simultaneously.

3) In general, for a certain number of histories, more accurate results will be obtained with more fictitious surfaces, however, the simulation will cost more time. The optimum solution of the sub-space division is hard to be determined. The sub-space division is relatively satisfied when the penetrating probability is close to 1/10 in every sub-space⁵.

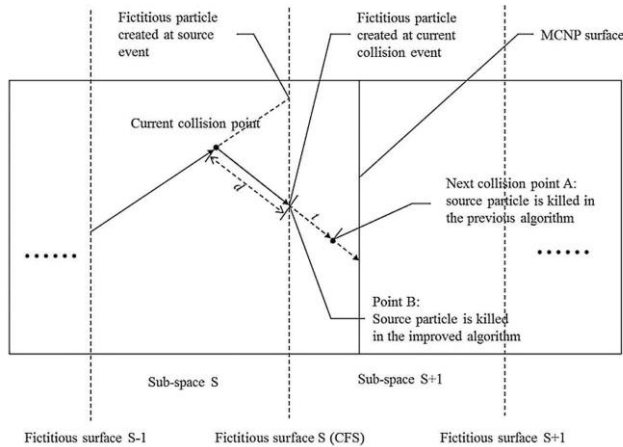


Fig.2. Particle transport in the CNP-AIS method

The procedure of the CNP-AIS method is as follows:

1) From source region to tally region, a series of neutron and photon fictitious surfaces are introduced to divide the whole geometry space into several sub-spaces. The total number of neutron and photon fictitious surfaces is K , and the number of sub-spaces is $K+1$. The fictitious surface k ($k=1,2,\dots,K$) is the CFS of sub-space k .

2) The Closest Photon Fictitious Surface (CPFS) and the Closest Neutron Fictitious Surface (CNFS) from the source are recorded.

3) The closest sub-space from the source is set to be current sub-space, in which the particles will be transported, and CFS is recorded. At least one of CPFS and CNFS is CFS. If CPFS and CNFS are at the same location, they are both set to be CFS.

4) The particles are transported from the source. At every source or collision event, fictitious particles are created on CPFS or CNFS using next event estimator according to the particle type.

5) When the source particle or secondary particle arrives at CFS, if the particle is neutron (or photon) and CNFS (or CPFS) is CFS, the particle will be killed; if not, its state will be stored and transport will be stopped on CFS.

It ensures that all the neutrons and photons will not traverse CFS.

6) After all the source particles are transported, the fictitious particles on CFS will be adjusted to be as many as the source particles using splitting/Russian roulette. These fictitious particles, source particles and secondary particles stored on CFS will be set as the source of the next sub-space. Then, the process will get back to step 1, and particle transport will be performed in the next sub-space.

When the closest fictitious surface of the same type as the particles is not CFS, the reason why the particles are stored and stopped on CFS in step 5 is shown in Fig. 3. If a neutron traverse CFS (CPFS) in sub-space S after collision event 1 and have collision event 2 which a secondary photon is generated, no photon fictitious particle will be created because the secondary photon is beyond CPFS. A neutron transport in the CNP-AIS method is shown in Fig.4.

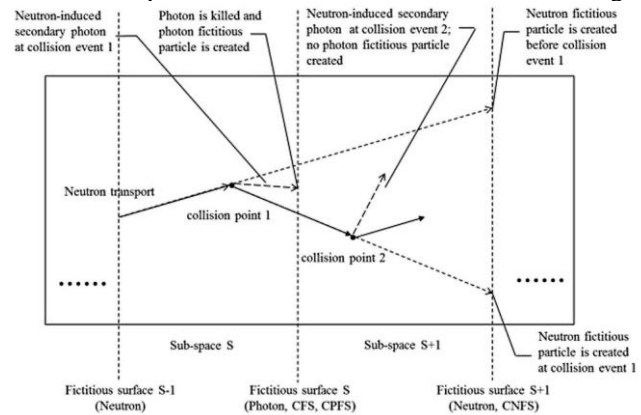


Fig.3. The situation when particle traversing CFS

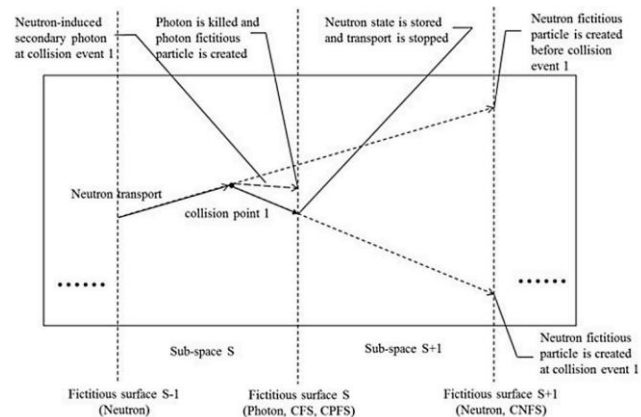


Fig.4. Particle transport in the NP-AIS method

In the NP-AIS method, except for the memory usage of analog Monte Carlo, additional memory should be allocated for the fictitious particles and source/secondary particles which are recorded on the fictitious surface. Because splitting/Russian roulette is used to adjust the number of fictitious particles, the space complexity of the NP-AIS method is $O(n)$, in which n represents the number of source particles.

B. FPAIS Method

For the Monte Carlo calculation of complex shielding structure like ducts and labyrinths, CNP-AIS cannot achieve efficient importance sampling. Therefore, FPAIS method was proposed to realize the automatic and efficient importance sampling. This method sets K guiding surface to guide particle transport. Fictitious particles are created on the guiding surface. The weight of fictitious particle is set according to the probability of scattering toward that guiding surface. The transport procedure is shown in Fig.5.

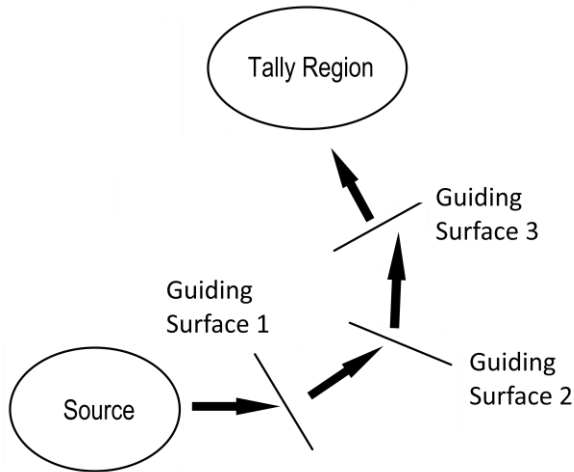


Fig.5. Particle transport in the FPAIS method

3. CAD Model to Monte Carlo Geometry Model Conversion Method

Due to the low efficiency of three-dimensional geometry, the CSG representation method used in Monte Carlo particle transport has become the bottleneck which limits the development of refined Monte Carlo simulation. CAD models are widely used in the design of nuclear facilities, which use BREP (Boundary Representation) to describe 3D solid models and has powerful geometric description capabilities. However, the difference between CSG representation and BREP prevents the use of CAD model in Monte Carlo particle transport.

In RShieldMC, one new BREP→CSG conversion method is implemented which completely splits the geometry based on geometry/topology information. This method uses the assistant surface generation strategy based on the characteristic of a convertible entity, which reduces the redundancy of the assistant surfaces, improves the conversion efficiency and simplifies the CSG expression. The efficiency of judging and selecting the splitting surfaces is improved by topology information. This method is implemented based on Open CASCADE Technology (OCCT) 3D modeling engine and can provide output file can be used in RShieldMC, Gean4 or MCNP.

4. Code Validation Test

After the development of the code, all functional modules of RShieldMC were tested and verified. A large number of examples including MCNP benchmark problems, our own problems and some international shield benchmark problems, for example, NUREG/CR-6115 PWR benchmark and NESDIP-2 Benchmark Experiment (ASPIS) were selected. An accelerator element model was used to test the BREP→CSG conversion method. The test of a homemade water tunnel radiation shielding problem and the NUREG/CR-6115 PWR benchmark are shown in this paper.

The accelerator element model is very complex, include a variety of screws, nuts and other fine structures, with 169 entities and 3084 faces which contains a lot of curved surfaces.

In the homemade water tunnel radiation shielding problem, the 3 MeV isotropic photon source is uniformly distributed in the water tunnel. The detectors are in the corner of the air cavity, as shown in the Fig. 6. And the photon cell fluxes in the detectors were calculated by using RShieldMC and MCNP5 code respectively, both without any variance reduction techniques. In MCNP5, MODE P E was used. The default setting of PHYS Card was used. The energy cut offs of photon and electron were both set as 1 eV. The parameters of RShieldMC was the same as those of MCNP5. As the length limit, only the result of the detector 4 was shown in this paper.

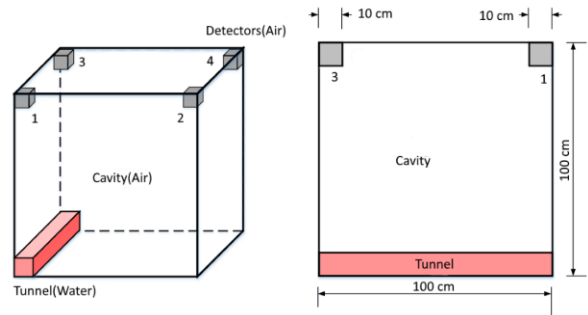


Fig. 6. The geometry of the water tunnel problem

NUREG/CR-6115 PWR pressure vessel fluence calculation benchmark problem issued by the NRC⁶ was calculated in this paper. The PWR model mainly consists of a 204 fuel assembly PWR core, a core barrel, thermal shield, vessel and an outer concrete biological shield. The power distribution is based on a detailed 15x15 fuel assembly pin-wise power distribution. The standard core loading pattern of the benchmark problems was used here. The azimuthal boundaries at 0 and 45 degrees were set to be reflecting boundaries. The outside of the biological shield wall, the top and bottom of the model were set to be void boundaries.

As shown in Fig.7, 6 cylinder surfaces were added to biological shield wall. The fluxes of these 6 cylinder

surfaces and the outer face of biological shield wall were tallied.

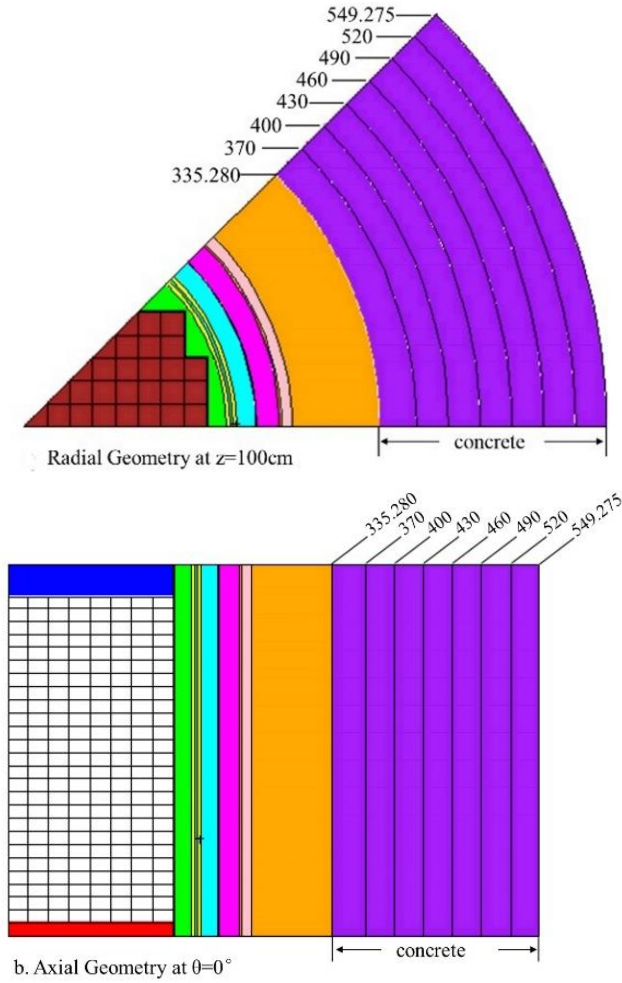


Fig.7. PWR model with full size biological shield wall (all dimensions in cm; the other parts of this model refer to Ref. 4)

Neutron/photon flux radial distribution in biological shield wall was calculated by using RShieldMC code with the methods of CNP-AIS and MCNP5 code with geometry splitting and Russian roulette respectively.

A figure of merit (FOM) was used to evaluate the computational efficiency. The FOM is defined as:

$$FOM = \frac{1}{R^2 \cdot T} \quad (1)$$

All these calculations were performed on a notebook computer with Intel Core i7-3520M CPU 2.90 GHz and 16.0 GB memory.

III. RESULTS

A. Conversion of the Accelerator Element Model

The results of the conversion of the accelerator element model are shown in Fig.8. The total conversion time is 344.04 seconds and the volume relative error through the conversion is 0.0135%, maintaining a high conversion accuracy and good conversion efficiency.

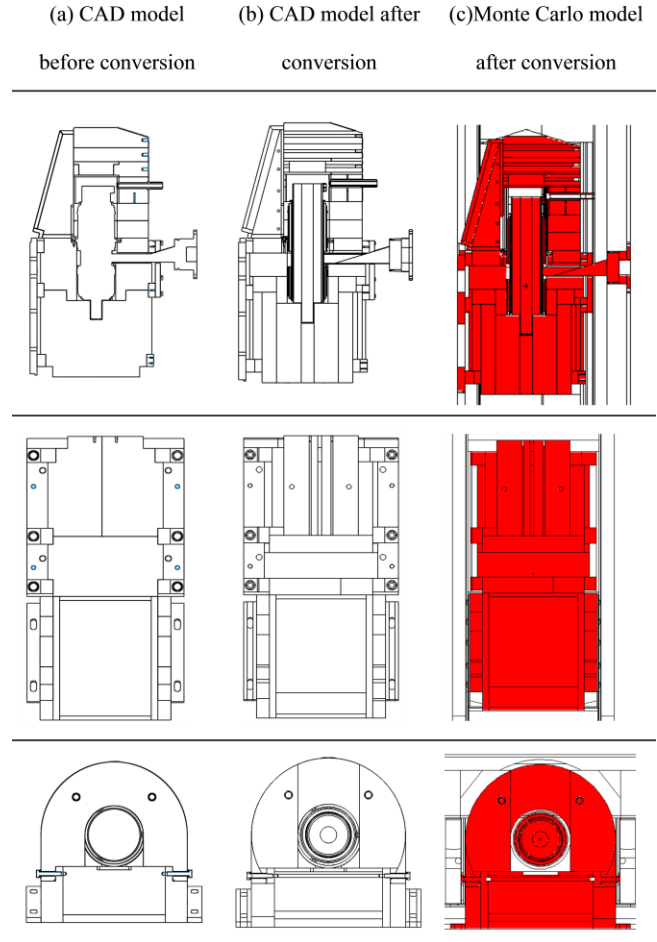


Fig.8. Cross-sectional view of the accelerator element.

B. The Water Tunnel Radiation Shielding Problem

In the water tunnel radiation shielding problem, the number of histories (NPS) was 5×10^8 . The computation time T was 3944 and 3365 minutes for MCNP5 and RShieldMC respectively.

The photon cell flux in increments of 0.5 MeV from 0.5 to 3 MeV are shown in Table I. The relative statistic errors of the fluxes are all below 3% for MCNP5 and RShieldMC. And the relative differences of MCNP5 and RShieldMC are also all below 3% at all energy bins. So the results of MCNP5 and RShieldMC are in good agreement. Additionally, the statistic errors are similar between the MCNP5 and RShieldMC with the same NPS. In consideration of their similar computation time, the efficiencies of MCNP5 and RShieldMC are similar in this problem.

C. NUREG/CR-6115 PWR Benchmark

In NUREG/CR-6115 PWR benchmark problems, for MCNP5 simulation, the number of histories (NPS) was 4×10^7 , and the computation time T was 1452 minutes.

In RShieldMC simulation, eleven neutron and photon cylindrical fictitious surfaces whose radii were 188, 215, 230, 340, 360, 390, 420, 450, 480, 510 and 530 cm, were introduced. NPS was 10^5 and T was 8 minutes.

the neutron flux results are shown in Table II and photon flux results are shown in Table III. MCNP5-GS represents MCNP5 code with geometry splitting and Russian roulette and RShieldMC-AIS represents RShieldMC code with CNP-AIS Method. R represents the estimated relative error.

The neutron and photon FOM curves of MCNP5-GS and RShieldMC-AIS are shown in Fig. 9 and Fig. 10.

As shown in Table II, for surface No. 1, 2, 3 and 4, the estimated relative errors of neutron results of MCNP5-GS and RShieldMC with CNP-AIS method are all below 10%, and the neutron results of MCNP5-GS and RShieldMC-AIS are in good agreement. For surface No. 5, 6 and 7, MCNP5-GS could not give reliable results, whereas the estimated relative errors of neutron results of RShieldMC-AIS are still below 10%. The neutron FOM curve of MCNP5-GS has an exponential decay with the surface radius increasing, because that the penetrating probability decreased through the concrete. However, the neutron FOM curve of

RShieldMC-AIS keeps stable approximately. The neutron FOMs of RShieldMC-AIS and MCNP5-GS for the first tally surface are similar, but the neutron FOM of RShieldMC for the sixth tally surface is increased by four orders of magnitude compared with that of MCNP5-GS. The similar performance for photon can be seen in Table III and Fig. 8. In this example, RShieldMC-AIS is much less time-consuming (only 8 minutes) than MCNP5-GS, but gives a much better performance.

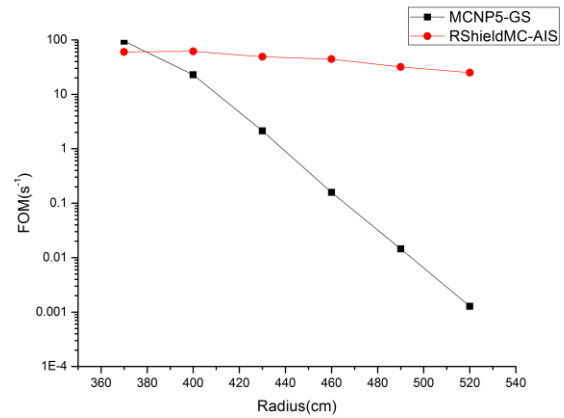


Fig.9. FOM curves of neutron flux radial distribution in biological shield wall.

Table I. Photon flux of detector 4 divided by energy bins

| Upper bound of the energy bin (MeV) | MCNP5 | | RShieldMC | | RShieldMC / MCNP5 Relative difference |
|-------------------------------------|--|-------|--|-------|---------------------------------------|
| | Flux per particle (n/cm ²) | R | Flux per particle (n/cm ²) | R | |
| 0.5 | 3.66E-09 | 1.10% | 3.77E-09 | 1.09% | 2.79% |
| 1 | 2.00E-09 | 1.49% | 2.00E-09 | 1.49% | 0.21% |
| 1.5 | 9.19E-10 | 2.20% | 9.18E-10 | 2.19% | 0.11% |
| 2 | 7.14E-10 | 2.49% | 7.16E-10 | 2.48% | 0.36% |
| 2.5 | 6.50E-10 | 2.61% | 6.55E-10 | 2.60% | 0.83% |
| 3 | 3.69E-08 | 0.35% | 3.71E-08 | 0.35% | 0.58% |

Table II. Neutron flux radial distribution in biological shield wall

| Surface No. | Radius (cm) | MCNP5-GS | | | RShieldMC-AIS | | |
|-------------|-------------|--|--------|----------|--|-------|----------|
| | | Flux per particle (n/cm ² ·s) | R | FOM | Flux per particle (n/cm ² ·s) | R | FOM |
| 1 | 370 | 1.80E-10 | 0.27% | 9.45E+01 | 1.88E-10 | 4.56% | 6.01E+01 |
| 2 | 400 | 1.36E-11 | 0.55% | 2.28E+01 | 1.39E-11 | 4.51% | 6.15E+01 |
| 3 | 430 | 9.06E-13 | 1.80% | 2.13E+00 | 9.44E-13 | 5.05% | 4.90E+01 |
| 4 | 460 | 6.78E-14 | 6.61% | 1.58E-01 | 6.32E-14 | 5.31% | 4.43E+01 |
| 5 | 490 | 3.04E-15 | 21.80% | 1.45E-02 | 4.36E-15 | 6.26% | 3.19E+01 |
| 6 | 520 | 3.09E-16 | 73.50% | 1.28E-03 | 3.07E-16 | 7.07% | 2.50E+01 |
| 7 | 549.275 | 0.00E+00 | - | - | 6.17E-18 | 8.67% | 1.66E+01 |

Table III. Photon flux radial distribution in biological shield wall

| Surface No. | Radius (cm) | MCNP5-GS | | | RShieldMC-AIS | | |
|-------------|-------------|--|--------|----------|--|-------|----------|
| | | Flux per particle (n/cm ² •s) | R | FOM | Flux per particle (n/cm ² •s) | R | FOM |
| 1 | 370 | 1.44E-10 | 0.26% | 1.02E+02 | 1.47E-10 | 3.80% | 8.66E+01 |
| 2 | 400 | 2.35E-11 | 0.45% | 3.40E+01 | 2.36E-11 | 3.88% | 8.30E+01 |
| 3 | 430 | 2.99E-12 | 1.03% | 6.49E+00 | 3.01E-12 | 3.68% | 9.23E+01 |
| 4 | 460 | 3.89E-13 | 2.74% | 9.17E-01 | 3.67E-13 | 4.52% | 6.12E+01 |
| 5 | 490 | 5.23E-14 | 6.49% | 1.64E-01 | 4.72E-14 | 3.06% | 1.33E+02 |
| 6 | 520 | 5.97E-15 | 18.90% | 1.94E-02 | 6.69E-15 | 2.42% | 2.13E+02 |
| 7 | 549.275 | 1.04E-15 | 25.00% | 1.10E-02 | 6.94E-16 | 2.58% | 1.88E+02 |

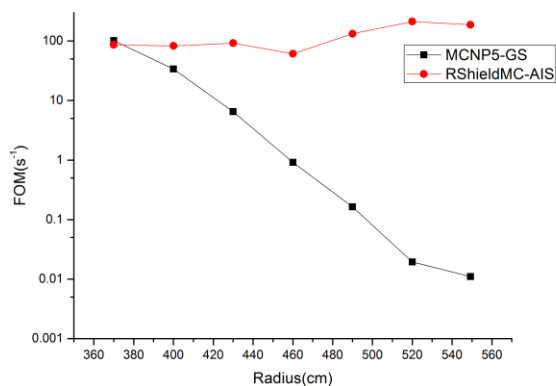


Fig.10. FOM curves of photon flux radial distribution in biological shield wall.

IV. CONCLUSIONS

In this study, a new Monte Carlo transport code called RShieldMC has been developed and validated. It supports coupled neutron/photon/electron transport, has some functions and tools especially for radiation shielding calculation. The BREP→CSG conversion method can convert CAD model to Monte Carlo geometry that RShieldMC can use directly. It has been validated and has a high conversion accuracy and good conversion efficiency. This method can greatly save the geometry modeling time in complex geometry shielding calculation.

To solve the deep penetration problem and complex shielding problem, two new variance reduction techniques called CNP-AIS and FPAIS methods are developed and implemented in RShieldMC.

The results of NUREG/CR-6115 PWR pressure vessel fluence calculation benchmark show that CNP-AIS method is applicable to different deep penetration problems, and improves the precision and efficiency of Monte Carlo method.

However, RShieldMC code is still in the testing phase. It needs to be validated using more benchmark problems. And some functions to be complemented and perfected, for example, implementing the proton transport and improve

the efficiency of neutron transport without any variance reduction methods.

ACKNOWLEDGMENTS

This work was supported by the subject of National Science and Technology Major Project of China (2013ZX06002001-007).

Simulations were carried out on the ‘Explorer 100’ cluster system of Tsinghua National Laboratory for Information Science and Technology, China.

REFERENCES

1. Will Schroeder, K.M., Bill Lorenson, “The Visualization Toolkit User's Guide”. Kitware, Inc (2005).
2. Pan Yuxi, Qiu Rui, Liu Liye, Ren Li, Zhu Huanjun, Li Junli, “Chinese Reference Human Voxel Phantoms for Radiation Protection: Development, Application and Recent Progress”, *Radiation Protection*, 2014(4),199-205(in Chinese).
3. Xin Wang, “Research on Key Method and Program Development of High Performance Monte Carlo Calculation of Radiation Shielding,” *Ph.D. Thesis*, Tsinghua University, Beijing (2016) (in Chinese).
4. J. Li, C. Li, and Z. Wu, “An Auto-Importance Sampling Method for Deep Penetration Problems,” *Progress in Nuclear Science & Technology*, 2:732-737 (2011).
5. J. J. Fan, “Research of Rare but Important Events Simulation in Monte Carlo Methods”, *Ph.D. Thesis*, Tsinghua University, Beijing (2004) (in Chinese).
6. J. F. Carew, “PWR and BWR pressure vessel fluence calculation benchmark problems and solutions,” Division of Engineering Technology, Office of Nuclear Regulatory Research, US Nuclear Regulatory Commission (2001).